

Article

The Effect of the Substituent Position on the Two-Photon Absorption Performances of Dibenzylideneacetone-Based Isomers

Liyun Zhao ¹, Yujin Zhang ¹, Hong Ma ^{2,*} and Jiancai Leng ^{1,*}

¹ School of Science, Qilu University of Technology, Jinan 250353, China; liyunzhao_mm@163.com (L.Z.); zhangyujin312@163.com (Y.Z.)

² School of Physics and Electronics, Shandong Normal University, Jinan 250014, China

* Correspondence: mahong@sdu.edu.cn (H.M.); jiancaileng@qlu.edu.cn (J.L.); Tel.: +86-531-8618-2521 (H.M.); +86-531-8963-1268 (J.L.)

Academic Editor: Qing-Hua Xu

Received: 31 October 2016; Accepted: 14 December 2016; Published: 20 December 2016

Abstract: The two-photon absorption and optical limiting properties of two dibenzylideneacetone derivatives with different substituent positions have been theoretically investigated by solving the coupled rate equations-field intensity equation in the nanosecond time domain using an iterative predictor-corrector finite-difference time-domain method. The calculations show that the electronic structure, the transition dipole moment, the energy gap between the highest occupied orbital (HOMO) and the lowest unoccupied orbital (LUMO), and the pumping rate for the two molecules are quite different due to the different position of chlorine atoms. Importantly, two-photon absorption and optical limiting properties of the molecules depend crucially on the substituent positions of the terminal group, indicating that subtle manipulation on the molecule can affect the nonlinear optical properties of the medium.

Keywords: two-photon absorption; optical limiting; dibenzylideneacetone derivatives; isomer

PACS: 33.80.-b; 31.15.A-

1. Introduction

Materials with excellent two-photon absorption (TPA) properties have attracted a tremendous amount of interest due to their versatile applications in frequency up-conversion lasing [1–3], 3-D microfabrication [4], two-photon fluorescence imaging [5], two-photon photodynamic therapy [6,7], and especially optical limiting (OL) [8–10]. Ideal OL materials show stronger nonlinear optical absorption when the intensity of incident laser increases. During the past few decades, with the widespread application of intense lasers as light sources, optical power limiting from hazards of the intense laser beam has become an urgent need for instrument protection, eye protection, and optical biology [11]. Therefore, it is an important task for researchers to design and synthesize optical limiters with a large TPA cross section [12,13].

TPA properties of the materials vary in the ability of intermolecular charge transfer, the strength of the donor/acceptor, the character of the conjugated bridge, and the extent of conjugation length [14–17]. At the same time, previous experimental studies have demonstrated that the substitute position of isomers can affect the distinct nonlinear optical properties [18–20]. However, to the best of our knowledge, theoretical investigations on the discrepancy of molecular dynamic TPA properties for isomers are rather insufficient. Most importantly, the consideration of laser-matter interaction on the dynamical nonlinear optical properties of the isomers is still in need, and nonlinear properties of the medium depend strongly on dynamical parameters of the interaction between light and matter, such as

the pulse intensity and the propagation distance of the pulse and the density of the medium should be considered.

Dibenzylideneacetone derivatives were reported to possess good TPA properties [21,22]. Furthermore, dibenzylideneacetone-based isomers exhibit different TPA and OL performances experimentally. In this paper, the TPA and OL properties of two dibenzylideneacetone derivatives with different substituent (chlorine group) positions, namely, (1E,4E)-1,5-bis(2-chlorophenyl)-1,4-pentadien-3-one(2-DCDBA) and (1E,4E)-1,5-bis(3-chlorophenyl)-1,4-pentadien-3-one(3-DCDBA) are investigated by solving the coupled rate equations and field intensity equation using an iterative predictor-corrector finite-difference time-domain (FDTD) method under nanosecond regimes. The effect of the substituent position on the nonlinear optical properties of these two derivatives is analyzed. In addition, the dynamical TPA cross sections of the compounds are obtained, and the influence of pulse or medium parameter on the dynamical TPA cross section is compared.

2. Theoretical Methods and Computational Details

2.1. Rate Equations and Field Intensity Equation

The rate equations for the populations of a three-level system can be written as [23]

$$\begin{aligned}\frac{\partial}{\partial t}\rho_{s_0} &= -\gamma_{s_0s_1}(\rho_{s_0} - \rho_{s_1}) - \gamma_{s_0s_2}(\rho_{s_0} - \rho_{s_2}) + \Gamma_{s_1}\rho_{s_1} \\ \frac{\partial}{\partial t}\rho_{s_1} &= \gamma_{s_0s_1}(\rho_{s_0} - \rho_{s_1}) - \gamma_{s_1s_2}(\rho_{s_1} - \rho_{s_2}) - \Gamma_{s_1}\rho_{s_1} + \Gamma_{s_2}\rho_{s_2} \\ \frac{\partial}{\partial t}\rho_{s_2} &= \gamma_{s_0s_2}(\rho_{s_0} - \rho_{s_2}) + \gamma_{s_1s_2}(\rho_{s_1} - \rho_{s_2}) - \Gamma_{s_2}\rho_{s_2}\end{aligned}\quad (1)$$

where Γ_{s_n} represents the decay rates of the S_n state, respectively. $\gamma_{s_0s_1}$ and $\gamma_{s_1s_2}$ denote the rates of the one photon induced transitions $S_0 \rightarrow S_1$ and $S_1 \rightarrow S_2$, which can be given by the one-photon absorption (OPA) cross sections $\sigma_{s_0s_1}$ and $\sigma_{s_1s_2}$ or dipole moments $d_{s_0s_1}$ and $d_{s_1s_2}$ in the rotating wave approximation (RWA).

$$\begin{aligned}\gamma_{s_0s_1}(t) &= \frac{|d_{s_0s_1}|^2 I(t)}{\hbar^2 c \epsilon_0} \frac{\Gamma}{\Omega_{s_0s_1}^2 + \Gamma^2} = \frac{\sigma_{s_0s_1} I(t)}{\hbar \omega} \frac{\Gamma^2}{\Omega_{s_0s_1}^2 + \Gamma^2} \\ \gamma_{s_1s_2}(t) &= \frac{|d_{s_1s_2}|^2 I(t)}{\hbar^2 c \epsilon_0} \frac{\Gamma}{\Omega_{s_1s_2}^2 + \Gamma^2} = \frac{\sigma_{s_1s_2} I(t)}{\hbar \omega} \frac{\Gamma^2}{\Omega_{s_1s_2}^2 + \Gamma^2} \\ \Omega_{s_0s_1} &= \omega - \omega_{s_0s_1}, \quad \Omega_{s_1s_2} = \omega - \omega_{s_1s_2}\end{aligned}\quad (2)$$

Similarly, the rate of two-photon induced transition $S_0 \rightarrow S_2$ can be calculated by the TPA absorption cross section $\sigma_{s_0s_2}$:

$$\gamma_{s_0s_2}(t) = \frac{\sigma_{s_0s_2} I^2(t)}{2\hbar \omega} \frac{\Gamma^2}{(2\omega - \omega_{s_0s_2})^2 + \Gamma^2} \quad (3)$$

where ω is the light frequency, and $I(t)$ is the intensity of the incident light field. Γ denotes the homogeneous broadening of the spectral line, which is set as $\hbar\Gamma = 0.1$ eV in our simulation [24].

As regards the electromagnetic field, the absorption of the field can be described by using the field intensity $I(t)$ [22]:

$$\left(\frac{\partial}{\partial z} + \frac{1}{c} \frac{\partial}{\partial t}\right) I(t) = -N[\sigma^{(1)} I(t) + \sigma^{(2)} I^2(t)] \quad (4)$$

where N is the molecular density. $\sigma^{(1)}$ and $\sigma^{(2)}$ are the total OPA and TPA cross sections, respectively, and they can be expressed as

$$\begin{aligned}\sigma^{(1)} &= \sigma_{s_0s_1}(\rho_{s_0} - \rho_{s_1}) + \sigma_{s_0s_2}(\rho_{s_1} - \rho_{s_2}) \\ \sigma^{(2)} &= \sigma_{s_0s_2}(\rho_{s_0} - \rho_{s_2})\end{aligned}\quad (5)$$

2.2. Static TPA Cross Section

Considering the transition characteristics of the molecule, the static maximum TPA cross section of the three-level system can be expressed as

$$\sigma_{STPA} \propto \frac{d_{s_0s_1}^2 d_{s_1s_2}^2}{(E_{s_0s_1} - E_{s_0s_2}/2)^2 \Gamma_f} + \frac{d_{s_0s_2}^2 (d_{s_2s_2} - d_{s_0s_0})^2}{(E_{s_0s_2}/2)^2 \Gamma_f} \quad (6)$$

where d_{mn} is the permanent dipole moment of state, and E_{mn} is the excitation energy. The final level broadening definition Γ_f defined as a common value of 0.1 eV. For the one-dimensional symmetrical structure of the molecule, the permanent dipole moments of the molecule are approximately equal to zero. Thus a simplified form can be obtained:

$$\sigma_{STPA} \propto \frac{d_{s_0s_1}^2 d_{s_1s_2}^2}{(E_{s_0s_1} - E_{s_0s_2}/2)^2 \Gamma_f} \quad (7)$$

2.3. Dynamical TPA Cross Section

Taking into account that the TPA coefficient β is related to the incident light intensity, we use a linear approximation to represent the TPA coefficient [23,24]:

$$\beta = \beta_0 - \xi I_0 \quad (8)$$

where β_0 is the static state TPA coefficient, and ξ is a constant. The reciprocal of the light intensity transmittance can be expressed as quadratic function of the input field intensity I_0 .

$$\frac{1}{T_z} = \frac{I_0}{I_z} = \exp(az) + \frac{[\exp(az) - 1]\beta}{\alpha} I_0 - \frac{[\exp(az) - 1]\xi}{\alpha} I_0^2 \quad (9)$$

where α is the linear absorption coefficient. The molecular TPA cross section σ_{tp} is related to β by

$$h\nu\beta = \sigma_{tp}N \quad (10)$$

where $h\nu$ is the incident photon energy. Therefore, we can obtain the dynamical TPA cross section by fitting the absorption coefficients.

3. Results and Discussion

Molecular structures of 2-DCDBA and 3-DCDBA are shown in Figure 1. The excitation energies of the excited states in the low energy region and transition dipole moments between the energy levels are calculated by using the time-dependent density functional theory (TDDFT) at the B3LYP/6-31G(d) level. The corresponding values are collected in Table 1. It is shown that both molecules can be simplified to a three-level system, including the ground state S_0 , the charge-transfer state S_1 , and the TPA state S_2 , as shown in Figure 1b. From state S_0 to state S_1 for both molecules, transition dipole moments differ by 0.4×10^{-30} C·m, while the state S_1 to state S_2 , the transition dipole moment differs by 0.31×10^{-29} C·m.

Table 1. Excitation energies and transition dipole moments of 2-DCDBA and 3-DCDBA.

Molecule	$E_{s_0s_1}$ /eV	$E_{s_1s_2}$ /eV	$d_{s_0s_1}/(10^{-29} \text{ C}\cdot\text{m})$	$d_{s_1s_2}/(10^{-29} \text{ C}\cdot\text{m})$
2-DCDBA	3.51	3.80	2.85	4.38
3-DCDBA	3.55	3.83	2.89	4.69

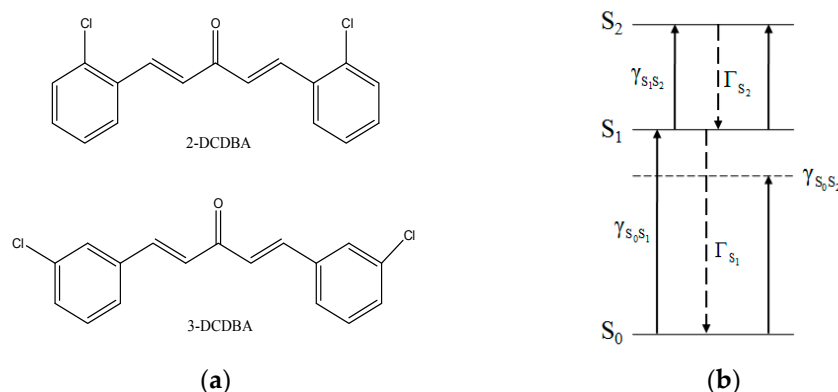


Figure 1. (a) Molecular structure diagrams of 2-DCDBA and 3-DCDBA; (b) scheme of the three-level theory model.

The incident pulse is modeled with a hyperbolic secant shape:

$$E(z, t = 0) = A_0 \text{sech}[1.76(z/c + z_0/c)/\tau] \cos[\omega(z + z_0/c)] \quad (11)$$

where A_0 is the peak amplitude of the input field, and τ is the full width at half maximum (FWHM) of the pulse intensity profile which is set to be 8 ns in our calculation. The selection of z_0 is to ensure that initial pulse into the medium is seldom at $t = 0$. In order to demonstrate the TPA behaviors, the frequency of the pulse ω is taken to be half of the two photon resonance frequency between states S_0 and S_2 , namely, $\omega = \omega_{S_0S_2}/2$. The decay rates of excited states Γ_{S_1} and Γ_{S_2} are assumed to be $1.0 \times 10^9/\text{s}$, $1.0 \times 10^{12}/\text{s}$, respectively [25]. The initial peak intensity is set as $1 \times 10^8 \text{ W/m}^2$. Before the laser pulse incident into the medium, all of the molecules are at ground state, that is, $\rho_{S_0}(t = 0) = 1$, $\rho_{S_1}(t = 0) = \rho_{S_2}(t = 0) = 0$.

The frontier orbitals and the energy gap between the highest occupied orbital (HOMO) and the lowest unoccupied orbital (LUMO) of 2-DCDBA and 3-DCDBA are depicted in Figure 2. It can be seen that the energy gap of 3-DCDBA (3.90 eV) is larger than that of 2-DCDBA (3.64 eV), which originates from the change in the substituent group position.

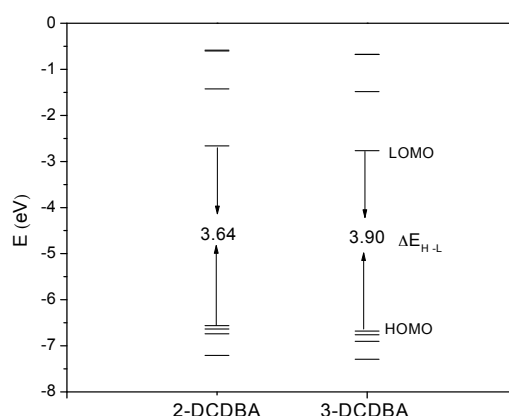


Figure 2. Molecular frontier orbital energy level diagram for 2-DCDBA and 3-DCDBA.

To explore the TPA properties of the two molecules, we give the transmittances of incident light field intensity for 2-DCDBA and 3-DCDBA at different propagation distances in Figure 3. It is evident that both mediums exhibit excellent nonlinear absorption ability. The transmittance is almost constant at low incident light intensity, suggesting that linear absorption plays a dominant role in this region. However, transmittance decreases rapidly with the increase in incident light intensity, which

originates from the TPA process in the three-level system. It is shown in Figure 3 that, for a certain molecule, the transmittance is smaller for a longer propagation distance because more energy of the field is transferred into the medium as pulse propagation. Obviously, transmittance for 3-DCDBA is much lower than that of 2-DCDBA, which means 3-DCDBA is preferred as an absorber. This result indicates that different positions of the chlorine substituent group lead to an influence on intensity transmittances, and the meta position is better than the ortho position.

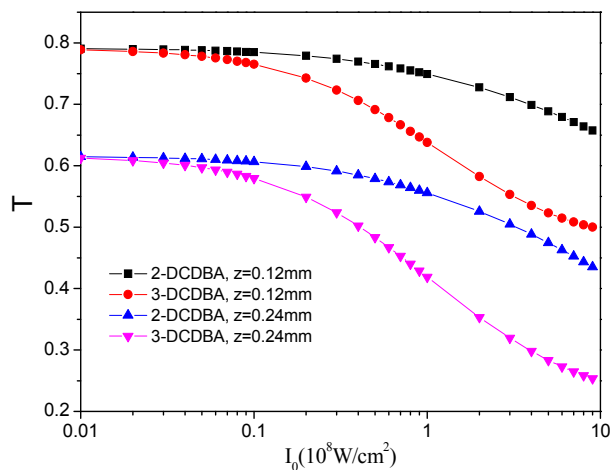


Figure 3. Field intensity transmittance as a function of the 2-DCDBA and 3-DCDBA incident light field at different propagation distances.

When the laser pulse propagates in the medium, the pulse strength envelope, the pump rate, and the particle number density of three levels are changed, as demonstrated in Figure 4. Figure 4a shows that pulse intensities are decreased in relation to pulse propagation process due to the interaction between the field and the medium, and the energy of the field is transferred into molecules. In addition, as shown in the figure, more energy is transferred for 3-DCDBA than that for 2-DCDBA during pulse propagation, which results from the substituent position. Figure 4b displays the pump rate of the TPA process for the molecules with a pulse intensity of $6 \times 10^8 \text{ W/cm}^2$ at $z = 0.24 \text{ mm}$. It is shown that the TPA rate of 3-DCDBA is much larger than that of 2-DCDBA, indicating that 2-DCDBA needs more time to become excited to a higher state. Figure 4c shows that most of the molecules are excited to the OPA state S_1 , while the TPA state S_2 is almost unpopulated. This phenomenon is understandable: the lifetime of state S_2 is on the picosecond scale, and populations on state S_2 will decay rapidly back to the state S_1 .

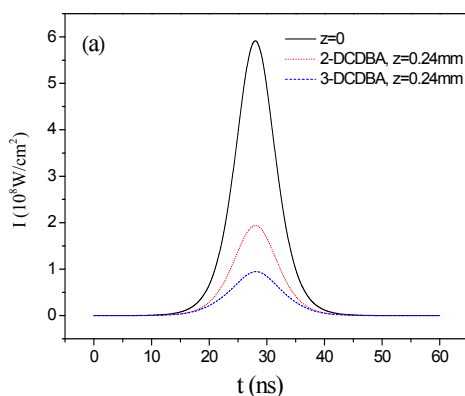


Figure 4. Cont.

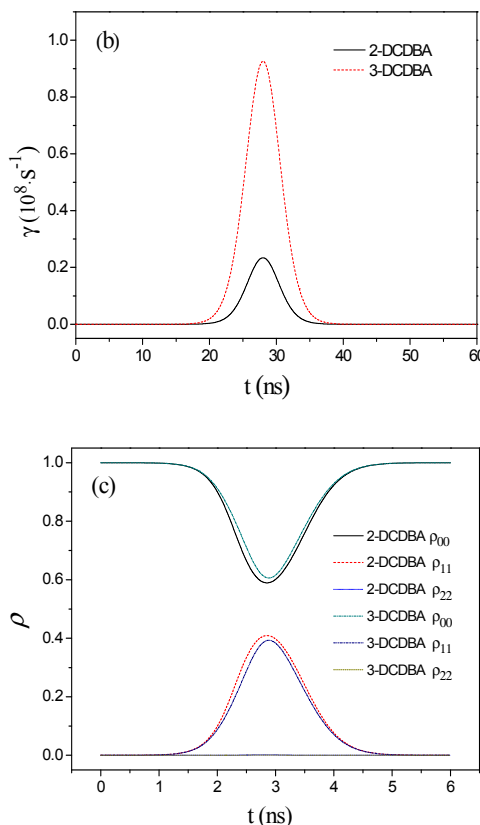


Figure 4. (a) The changes in the pulse intensity envelope; (b) the pump rate ($I = 6 \times 10^8 \text{ W/cm}^2$, $z = 0.24 \text{ mm}$); and (c) the particle number density of three levels for 2-DCDBA and 3-DCDBA ($I = 6 \times 10^8 \text{ W/cm}^2$, $z = 0.24 \text{ mm}$).

The curves of output fluence versus input fluence for both mediums at different propagation distances and particle number densities are shown in Figure 5. One can see that input fluence significantly decrease with the increase in propagation distances and particle number densities. It is obvious that, with the increase in the medium length and particle number densities, more energy of the field is absorbed due to the interaction between the field and the medium. This suggests that the OL performance is more apparent for longer propagation distance and larger particle number densities, leading to an enhancement in the OL abilities. Consistent with previous conclusions, the OL performance of 3-DCDBA is much stronger than that of 2-DCDBA.

Based on the input–output peak intensity relation, we obtained dynamical TPA cross sections of 2-DCDBA and 3-DCDBA at propagation distances of 0.12 mm and 0.24 mm, as shown in Table 2. Calculation results show that the values of the TPA coefficient β and the dynamical TPA cross section σ_{tp} for both molecules increase with the increase in propagation distances, and the TPA cross section of 3-DCDBA is larger than the 2-DCDBA at different propagation distances. Therefore, the values of the TPA cross section depend crucially on the thickness of the medium. Compared with the static TPA cross sections of 2-DCDBA and 3-DCDBA, which are 356 GM ($1 \text{ GM} = 10^{-50} \text{ cm}^4\text{s/photon}$) and 396 GM, respectively, the dynamical TPA cross sections are two orders of magnitude larger. This is because the dynamical TPA cross section has taken the two-step TPA process into consideration, while the static TPA cross section only includes the contribution of the one-step TPA. In the case of both static and dynamical conclusions, 3-DCDBA has a larger TPA cross section compared with 2-DCDBA, showing that the nonlinear absorption performance of 3-DCDBA is better than that of 2-DCDBA due to the different position of the substituent group.

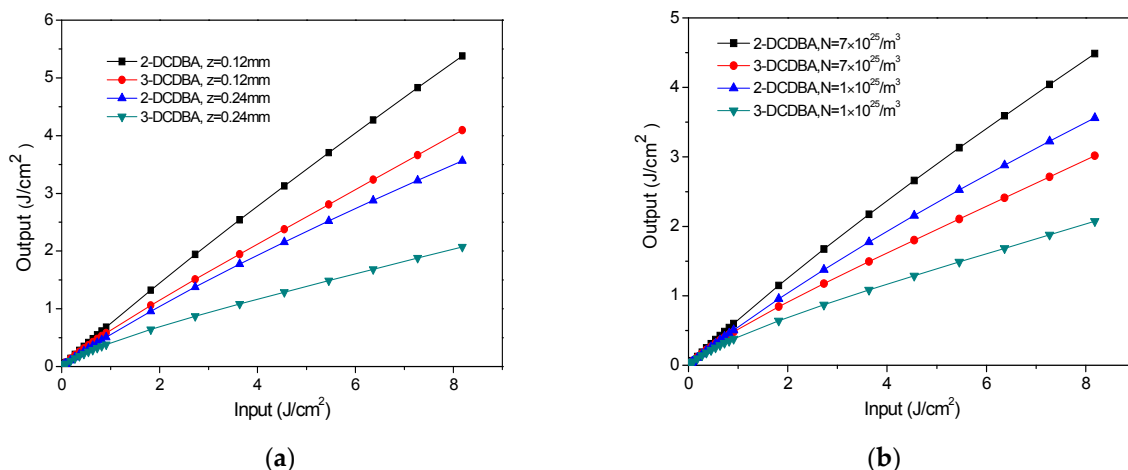


Figure 5. Optical limiting behaviors of 2-DCDBA and 3-DCDBA at (a) different propagation distances ($N = 1 \times 10^{25}/\text{m}^3$) and (b) different particle number densities ($z = 0.24$ mm).

Table 2. The values of linear absorption coefficient α (10^3 m/W), the TPA coefficient β (nm/W), dynamical TPA cross section σ_{tp} (10^5 GM), and the static TPA cross section (GM) of 2-DCDBA and 3-DCDBA at different propagation distances.

Molecule	z	α	β_0	σ_{tp}	σ_{STPA}
2-DCDBA	0.12 mm	1.98	0.40	1.23	366
	0.24 mm	1.04	0.81	2.48	
3-DCDBA	0.12 mm	4.09	0.89	2.72	396
	0.24 mm	2.22	1.92	5.90	

4. Conclusions

Dynamical analysis of optical limiting and TPA activities of two dibenzylideneacetone derivatives 2-DCDBA and 3-DCDBA were studied using the dynamical nonlinear absorption theory of nanosecond laser pulses. Our numerical results show that electronic structures, transition dipole moments, HOMO–LUMO energy gaps, and pump rates are influenced by the position of the substituent group, and 3-DCDBA, with the position of the substituent group at the meta position, has preferable nonlinear absorption properties, with a change in propagation distance and particle number density of the medium. This indicates that TPA and OL properties of the molecules depend crucially on the substituent positions of the terminal group, and subtle manipulation on the molecule can affect the nonlinear optical properties of the medium. Our theoretical results explain that the difference in nonlinear optical properties for the isomers and provide insight on the design of organic molecules with good TPA properties.

Acknowledgments: The authors acknowledge the financial support from the General Program of the National Nature Science Foundation of China under Grant No. 11304172, and No. 11304186. This work was also supported by Funding of Shandong Province Key Research Development Program, China (2015GGX101017), Qilu University of Technology Subject Construction Funds, China, the Excellent Young Scholars Research Fund of Shandong Normal University, China, and the International Cooperation Training Program for Young and Middle School Teachers in Shandong Province, China.

Author Contributions: Jiancai Leng and Hong Ma suggested the project; Liyun Zhao, Yujin Zhang carried out the theoretical simulations. Liyun Zhao wrote the draft paper. All authors discussed and revised the results.

Conflicts of Interest: The authors declare no conflict of interest.

References

1. Lin, T.C.; Tsai, B.K.; Huang, T.Y.; Chien, W.; Liu, Y.Y.; Li, M.H.; Tsai, M.Y. Synthesis and two-photon absorption properties of truxene-cored chromophores with functionalized pyrazine units fused as the end-groups. *Dyes Pigments* **2015**, *120*, 99–111. [[CrossRef](#)]
2. Tian, G.J.; Xiang, N.; Zhou, H.T.; Li, Y.R.; Li, B.; Wang, Q.C.; Su, J.H. A novel D-A-D-A-D type molecule based on substituted dihydroindolo [3, 2-b] carbazole with large two-photon absorption cross section and excellent aggregation-induced enhanced emission property. *Tetrahedron* **2016**, *72*, 298–303. [[CrossRef](#)]
3. Fang, H.H.; Chen, Q.D.; Yang, J.; Xia, H.; Ma, Y.G.; Wang, H.Y.; Sun, H.B. Two-photon excited highly polarized and directional upconversion emission from slab organic crystals. *Opt. Lett.* **2010**, *35*, 441–443. [[CrossRef](#)] [[PubMed](#)]
4. Erskine, L.L.; Heikal, A.A.; Kuebler, S.M.; Rumi, M.; Wu, X.; Marder, S.R.; Perry, J.W. Two-photon polymerization initiators for three- dimensional optical data storage and microfabrication. *Solid State Phys.* **1999**, *398*, 51–54.
5. Denk, W.; Strickler, J.H.; Webb, W.W. Two-photon laser scanning fluorescence microscopy. *Science* **1990**, *248*, 73–76. [[CrossRef](#)] [[PubMed](#)]
6. Kim, S.; Ohulchanskyy, T.Y.; Pudavar, H.E.; Pandey, R.K.; Prasad, P.N. Organically modified silica nanoparticles co-encapsulating photosensitizing drug and aggregation-enhanced two-photon absorbing fluorescent dye aggregates for two-photon photodynamic therapy. *J. Am. Chem. Soc.* **2007**, *129*, 2669–2675. [[CrossRef](#)] [[PubMed](#)]
7. Khurana, M.; Collins, H.A.; Karotki, A.; Anderson, H.L.; Cramb, D.T.; Wilson, B.C. Quantitative in vitro demonstration of two-photon photodynamic therapy using photofrin[®] and visudyne[®]. *Photochem. Photobiol.* **2007**, *83*, 1441–1448. [[CrossRef](#)] [[PubMed](#)]
8. Ehrlich, J.E.; Wu, X.L.; Lee, I.Y.S.; Hu, Z.Y.; Röckel, H.; Marder, S.R.; Perry, J.W. Two-photon absorption and broadband optical limiting with bis-donor stilbenes. *Opt. Lett.* **1997**, *22*, 1843–1845. [[CrossRef](#)] [[PubMed](#)]
9. Ma, H.; Leng, J.C.; Liu, M.; Zhao, L.N.; Jiao, Y. Theoretical investigation of two-photon absorption properties and optical limiting behavior of two symmetrical fluorene derivatives. *J. Nonlinear Opt. Phys. Mater.* **2015**, *24*, 1550046. [[CrossRef](#)]
10. Zhao, L.Y.; Zhang, Y.J.; Ma, H.; Leng, J.C. Influence of terminal group on nonlinear optical properties of fluorene derivatives. *Acta Phys. Chim. Sin.* **2016**, *32*, 1543–1548.
11. Patila, P.S.; Dharmaprakasha, S.M.; Ramakrishna, K.; Fun, H.K.; Kumard, R.S.S.; Rao, D.N. Second harmonic generation and crystal growth of new chalcone derivatives. *J. Cryst. Growth* **2007**, *303*, 520–524. [[CrossRef](#)]
12. Yao, C.B.; Zhang, Y.D.; Li, J.; Chen, D.T.; Yin, H.T.; Yu, C.Q.; Yuan, P. Study of the nonlinear optical properties and behavior in phenoxy-phthalocyanines liquid at nanosecond laser pulses. *Opt. Mater.* **2014**, *37*, 80–86. [[CrossRef](#)]
13. Gary-Bobo, M.; Mir, Y.; Rouxel, C.; Brevet, D.; Basile, I.; Maynadier, M.; Vaillant, O.; Mongin, O.; Blanchard-Desce, M.; Morère, A.; et al. Mannose-functionalized mesoporous silica nanoparticles for efficient two-photon photodynamic therapy of solid tumors. *Angew. Chem.* **2011**, *50*, 11425–11429. [[CrossRef](#)] [[PubMed](#)]
14. Avirah, R.R.; Jayaram, D.T.; Adarsh, N.; Ramaiah, D. Squaraine dyes in PDT: From basic design to in vivo demonstration. *Org. Biomol. Chem.* **2012**, *10*, 911–920. [[CrossRef](#)] [[PubMed](#)]
15. Harvey, P.D.; Gan, L.; Aubry, C. Charge transfer emissive singlet excited states and photoinduced electron transfer properties in the diarylideneacetone compounds (RCHCH)₂CO; R = phenyl, 1- and 2-naphthyl, 3-(N-ethylcarbazoyl), and 4-(C₅H₅)Fe(C₅H₄C₆H₄CHCH(CO)CHCHC₆H₅). *Can. J. Chem.* **1990**, *68*, 2278–2288. [[CrossRef](#)]
16. Albota, M.; Beljonne, D.; Brédas, J.L.; Ehrlich, J.E.; Fu, J.Y.; Heikal, A.A.; Hess, S.E.; Kogej, T.; Levin, M.D.; Marder, S.R.; et al. Design of organic molecules with large two-photon absorption cross sections. *Science* **1998**, *281*, 1653–1656. [[CrossRef](#)] [[PubMed](#)]
17. Ma, H.; Leng, J.C.; Liu, M.; Zhao, L.N.; Jiao, Y. Two-photon absorption and optical limiting of a fluorenyl-based chromophore with femtosecond laser pulse. *Opt. Commun.* **2015**, *350*, 144–147. [[CrossRef](#)]

18. Arnbjerg, J.; Jiménez-Banzo, A.; Paterson, M.J.; Nonell, S.; Borrell, J.I.; Christiansen, O.; Ogilby, P.R. Two-photon absorption in tetraphenylporphycenes: Are porphycenes better candidates than porphyrins for providing optimal optical properties for two-photon photodynamic therapy? *J. Am. Chem. Soc.* **2007**, *129*, 5188–5199. [[CrossRef](#)] [[PubMed](#)]
19. Guillaume, M.; Ruud, K.; Rizzo, A.; Monti, S.; Lin, Z.; Xu, X. Computational study of the one- and two-photon absorption and circular dichroism of (L)-tryptophan. *J. Phys. Chem. B* **2010**, *114*, 6500–6512. [[CrossRef](#)] [[PubMed](#)]
20. Nguyen, K.A.; Day, P.N.; Pachter, R. One- and two-photon spectra of platinum acetylide chromophores: A TDDFT study. *J. Phys. Chem. A* **2009**, *113*, 13943–13952. [[CrossRef](#)] [[PubMed](#)]
21. Aditya, P.; Kumar, H.; Kumar, S.; Rajashekar; Muralikrishna, M.; Muthukumar, V.S.; Kumar, B.S.; Sai, S.S.S.; Rao, G.N. Novel D- π -A- π -D type organic chromophores for second harmonic generation and multi-photon absorption applications. In Proceedings of the International Conference on Recent Trends in Applied Physics and Material Science, Rajasthan, India, 1–2 February 2013; AIP Publishing: New York, NY, USA, 2013; Volume 1536, pp. 751–752.
22. Kiran, J.A.; Chandrasekharan, K.; Nooji, S.R.; Shashikala, H.D.; Umesh, G.; Kalluraya, B. X(3) measurements and optical limiting in dibenzylideneacetone and Its derivatives. *Chem. Phys.* **2006**, *324*, 699–704. [[CrossRef](#)]
23. Wang, C.K.; Zhao, P.; Miao, Q.; Sun, Y.P.; Zhou, Y. Optical limiting and dynamical two-photon absorption of organic compounds for a nanosecond pulse. *J. Phys. B At. Mol. Opt. Phys.* **2010**, *43*, 39–41. [[CrossRef](#)]
24. Gel'mukhanov, F.; Baev, A.; Macák, P.; Luo, Y.; Ågren, H. Dynamics of two-photon absorption by molecules and solutions. *J. Opt. Soc. Am. B* **2002**, *19*, 937–945. [[CrossRef](#)]
25. Gavriluk, S.; Polyutov, S.; Jha, P.C.; Rinkevicius, Z.; Ågren, H.; Gel'mukhanov, F. Many-photon dynamics of photobleaching. *J. Phys. Chem. A* **2007**, *111*, 11961–11975. [[CrossRef](#)] [[PubMed](#)]



© 2016 by the authors; licensee MDPI, Basel, Switzerland. This article is an open access article distributed under the terms and conditions of the Creative Commons Attribution (CC-BY) license (<http://creativecommons.org/licenses/by/4.0/>).